석사학위논문

Design of Tri-Band Branch Line Coupler Using CRLH

삼중대역 CRLH 전력분배기 설계

2016.08.22

Graduate School of

Chonbuk National University

Division of Electronics and Information Engineering

Qi Wang

Design of Tri-Band Branch Line Coupler Using CRLH

삼중대역 CRLH 전력분배기 설계

2016.08.22

Graduate School of

Chonbuk National University

Division of Electronics and Information Engineering

Qi Wang

Design of Tri-Band Branch Line Coupler Using CRLH

Academic Advisor: Professor Yongchae Jeong

A Dissertation Submitted in Partial Fulfillment of the Requirements
for the Degree of
Masters of Science in Electronic Engineering

2016.05.09

Graduate School of Chonbuk National University
Division of Electronics and Information Engineering

Qi Wang

The Master dissertation of Qi Wang
is approved by

Chair, Professor, Hae-Won Son
Chonbuk National University

Professor, Donggu Lim
Chonbuk National University

Advisor, Professor, Yongchae Jeong
Chonbuk National University

2016. 06. 20

Graduate School of
Chonbuk National University

Dedication

This thesis is dedicated to my parents.

For their endless love, support and encouragement.

-Author

Contents

List of Figures

List of Tables

Abbreviations

MTM: Metamaterial

TL: Transmission Line

LH: Left-Handed

RH: Right-Handed

CRLH: Composited Right/Left Handed

D-CRLH: Dual-CRLH

DL-CRLH: Double-Lorentz CRLH

BLC: Branch Line Coupler

DB: Dual-Band

TB: Tri-Band

LE: Lumped Element

BPF: Band Pass Filter

ABSTRACT

Qi Wang

Electronics and Information Engineering Department

Graduate School

Chonbuk National University

In this paper, the design of a compact tri-band (TB) branch line coupler (BLC) using a modified double-Lorentz (DL) composite right/left handed (CRLH) transmission line (TL) is described. By properly choosing the parameters of the DL CRLH TLs, the unit structure yields phase responses of $-\pi/4$, $\pi/4$ and $-\pi/4$ at three arbitrary operating frequencies. Employing this structure, a TB microstrip BLC operating at 0.195 GHz, 0.67 GHz and 1.465 GHz is achieved. The size of the proposed TB BLC is significantly compact, at 14.2% of the previous TB BLC when they are both designed using DL CRLH TLs for the same TB frequencies. As a result, the proposed TB BLC has a more compact size than that of the previous work by adopting new TB phase relationships. Simulated and measured results show good agreement, and the operating frequencies in all 3 bands are well attained. This proposed TB BLC is significantly compact, and has steady performances due to the reliable realization, which is very useful in practical applications.

Keywords: Tri-band, Branch Line Coupler, CRLH.

Student ID Number: 201450825

Chapter 1

Introduction

This chapter introduced basic concepts and developments about CRLH and main contributions of this thesis.

1.1 Literature review

Metamaterials (MTMs) became a very actual topic in the present research interest field, due to their unusual but interesting characteristics, not encountered in nature [1]. Metamaterials are artificial structures that can be designed to exhibit specific electromagnetic properties not commonly found in nature. Recently, metamaterials with simultaneously negative permittivity (ε) and permeability (μ), more commonly referred to as left-handed (LH) materials, have received substantial attention in the scientific and engineering communities. Science magazine even named LH materials (LHMs) as one of the top ten scientific breakthroughs of 2003 [2].

A CRLH transmission line is the expansion of the PLH because it includes a series inductance and a parallel capacitance, which always exist in the practical LC-network implementation of the PLH transmission line. The CRLH TL can be used in dual band (DB) device design because of its nonlinear characteristic of phase [4].

As a dual concept of the conventional CRLH TL, the dual composite

right/left-handed (D-CRLH) transmission line metamaterial was introduced and its properties were investigated by Caloz [5]. The practical artificial LC-network implementation of the D-CRLH transmission line always accompanies parasitic elements (a series inductance and a parallel capacitance) and these parasitic elements are regarded as important transmission line parameters; the novel transmission line metamaterial is referred as a double-Lorentz (DL) transmission line [6]. A DL TL metamaterial has an intrinsic tri-band property that can be used in tri-band microwave components. Tri-band components are salutary to reduce the size of devices used in recent multiband mobile communication systems. In wireless communication circuits, branch-line coupler (BLC) is used for dividing an input signal into two output signals with 90° phase difference. The conventional BLC made by λ/4 right-handed (RH) TL operates at a target frequency f_1 and at its odd harmonics [7]. However, wireless systems may demand arbitrary second or third operating frequencies, which are not a multiple of f_1. The BLC using DL TLs can be a solution of such problems because of its operation at arbitrary three frequency bands. In this article, we present fundamental properties of DL TL and possible applications, including their results.

A concept and theory of size reduction was proposed in [8] for CRLH DB BLC design. In that paper, the positive phase response, namely LH range phase was chosen to design the DB BLC. As a result, the circuit size of DB BLC was reduced and the new BLC was only 34.4% of the previous DB BLC [4] in size. In this thesis, LH range phase is also chosen for DL CRLH TB BLC design to reduce the circuit size. The TB theory is analyzed and the experimental results prove this approach is available in designing a compact TB BLC.

1.2 Thesis contributions

This thesis has the following contributions on CRLH tri-band theory analysis, circuit size reduction of tri-band devices.

In terms of TB BLC designed by DL CRLH, the previous research showed that the circuit had a bulky size. In order to reduce the circuit size, another pair of phase responses ($-\pi/4$, $\pi/4$, $-\pi/4$) are chosen in this work in which one of them is positive (LH range).

Usually, the LH range phases are not chosen because it is strongly dependent on the LH part of CRLH TL. The LH TL realized by lumped elements is not perfect homogenous material as a result it may lead to some error. In this paper, this problem is solved by analyzing the overall circuit model of DL-CRLH and through *S*-parameters, which are obtained from ABCD matrix, thus phase responses can be derived. This derived phase is accurate and it can be used to exam the error and optimize the phase performance.

1.3 Thesis organization

This thesis is organized as follows, Chapter 2 is for basic concept and characteristic of CRLH. Following Chapter 3 introduces BLC and describes the principle of multiband BLC design and size reduction theory of CRLH TL . DL CRLH and tri-band BLC design is in Chapter 4. Chapter 5 presents general conclusions and outlook.

Chapter 2

Basic Concepts of CLRH

This chapter introduced basic concepts and developments about CRLH and main contributions of this thesis.

2.1 Ideal Homogeneous CRLH TLs

A homogeneous TL is perfectly uniform, i.e., a TL that has invariant cross section along the direction of propagation [3]. The TL is in addition called ideal if it can transmit signals at all frequencies, from zero to infinity. Fig. 2.1 shows a representation of an ideal homogeneous TL.

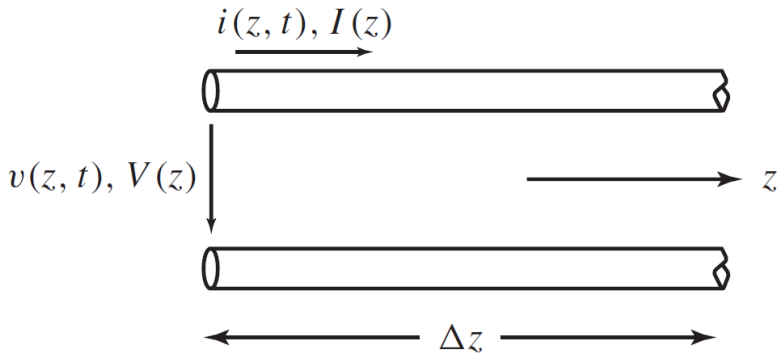

Figure 2.1 Representation of an ideal homogeneous (perfectly uniform) TL in the form of its incremental model (length $z \rightarrow 0$) with time domain or steady-state voltage/currents, $v(z, t)/i(z, t)$ and $V(z)/I(z)$, respectively.

Although RH homogeneous TLs are commonly used (e.g., coaxial or microstrip lines), LH or CRLH homogeneous TLs do not seem to be possible, due to the unavailability of real homogeneous LH or CRLH materials. However, it is possible to construct effectively homogeneous artificial LC TL structures, or MTM TLs, that perfectly mimic ideal TLs in a restricted range of frequencies. Despite the nonexistence of ideal homogeneous CRLH TLs, the analysis of such TLs is extremely useful because it provides insight regarding the fundamental aspects of CRLH MTMs with very simple relations and, more importantly, because it really describes the fundamental characteristics of MTMs due to their effective-homogeneity. The difference between a perfectly homogeneous TL and an effectively homogeneous TL is that in the former case we have an incremental length $\Delta z \to 0$, whereas in the latter case we must consider the restriction

$$\Delta z \square \ \lambda_g \text{ (at least } \Delta z < \frac{\lambda_g}{4})$$

where λ_g represents the guided wavelength and Δz is typically equal the average unit cell size p^2.

2.2 RH-TL and LH-TL

The equivalent circuits of a cell, for RH-TL and LH-TL are shown in Fig. 2.2

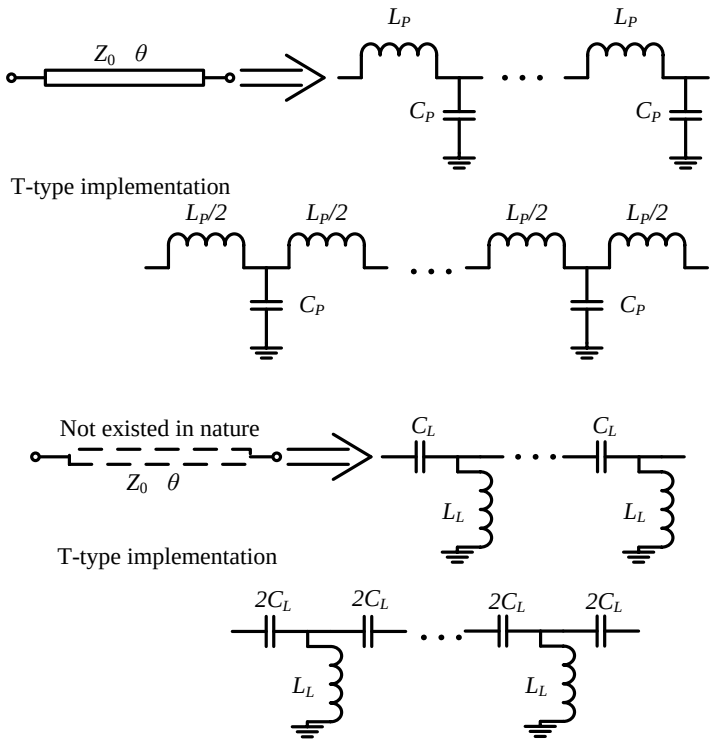

Figure 2.2 Unit cells for RH TL and LH TL

In these circuits, L_R, C_R and L_L, C_L are the distributed inductance and capacitance for RH-TL and LH-TL respectively. For these equivalent circuits, the propagation constant and the characteristic impedance can be determined with the following formulas:

$$\gamma = \sqrt{Z'(\omega)Y'(\omega)} = \alpha + j\beta \tag{2.1}$$

$$Z_C = \sqrt{\frac{Z'(\omega)}{Y'(\omega)}} \tag{2.2}$$

respectively, where $Z'(\omega)$ and $Y'(\omega)$ are the impedance of the series branch and the admittance of the parallel branch, is the attenuation constant and β is the phase constant.

If the line is lossless ($\alpha = 0$), then the propagation constant is pure imaginary, while the impedance is pure real. For RH-TL we can write (Fig. 2.2):

$$Z'(\omega) = j\omega L_R', Y'(\omega) = j\omega C_R' \quad (2.3a,b)$$

By inserting (2 .3a, b) in (2.1) and (2.2), we get:

$$\beta = \omega\sqrt{L_R' C_R'} > 0, Z_C = \sqrt{\frac{L_R'}{C_R'}} \quad (2.4a,b)$$

For LH-TL, it may be written (Fig. 2.2):

$$Z'(\omega) = \frac{1}{j\omega C_L'}, Y'(\omega) = \frac{1}{j\omega C_L'} \quad (2.5a,b)$$

By inserting (2.5 a, b) in (2.1) and (2.2), we get:

$$\beta = -\frac{1}{\omega\sqrt{L_L' C_L'}} < 0, Z_C = \sqrt{\frac{L_L'}{C_L'}} \quad (2.6a,b)$$

The equations (2.4a) and (2.6a) are the dispersion equations for RH-TL and LH-TL, respectively. The qualitative graphic representation of these equations is given in Fig. 2.3.

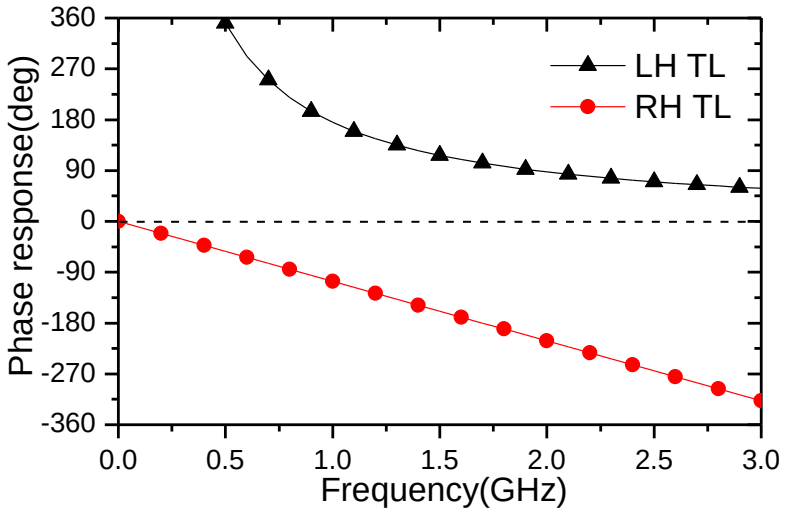

Figure 2.3 The phase responses of a LH TL and RH TL

The phase velocity, $v_p = \omega/\beta$ obtained from the dispersion equations (2.4a) and (2.6a) is positive for RH-TL and negative for LH-TL. The group velocity, $v_g = 1/(d\beta/d\omega)$, is positive for both RH-TL and LH-TL. Therefore, the energy transport is, from generator to load in both cases, but for LH-TL, due to the fact that the phase velocity is negative, the wave is propagated backwards (from load to generator).

2.3 CRLH TLs

As mentioned above, the equivalent circuit of CRLH-TL is a combination of the equivalent circuits for RH-TL and LH-TL. The equivalent circuit for CRLH-TL is given in Fig. 2.4, where, similar to RH-TL and LH-TL, Δz must be small enough compared to the wavelength.

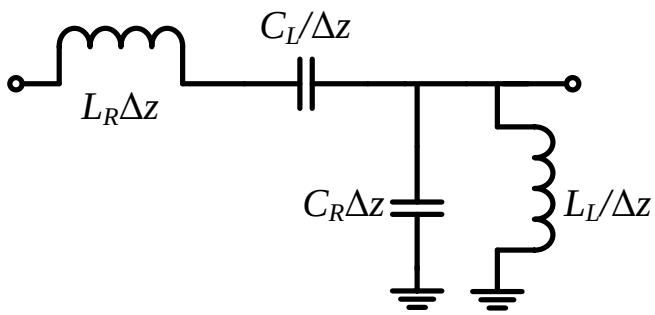

Figure 2.4 The unit cell of CRLH TL

For the circuit given in Fig.3:

$$Z' = j\left(\omega L'_R - \frac{1}{\omega C'_L}\right) \tag{2.7}$$

$$Y' = j\left(\omega C'_R - \frac{1}{\omega L'_L}\right) \tag{2.8}$$

Using (2.7) and (2.8), with the relations (2.1) and $\alpha = 0$ (lossless circuit), we get:

$$\beta = -j\sqrt{Z'Y'} = -j\sqrt{j^2\left(\omega L'_R - \frac{1}{\omega C'_L}\right)\left(\omega C'_R - \frac{1}{\omega L'_L}\right)}$$

$$= s(\omega)\sqrt{\omega^2 L'_R C'_R - \frac{L'_R}{L'_L} - \frac{C'_R}{C'_L} + \frac{1}{\omega^2 C'_L L'_L}}$$

$$= s(\omega)\sqrt{\omega^2 L'_R C'_R - \frac{L'_R C'_L + L'_C L'_R}{C'_L L_L{}'} + \frac{1}{\omega^2 C'_L L'_L}}$$

$$= s(\omega)\sqrt{\left(\frac{\omega}{\omega'_R}\right)^2 + \left(\frac{\omega'_L}{\omega}\right)^2 - k\omega_L'^2}, \qquad (2.9)$$

where $\begin{cases}\omega'_R = 1/\sqrt{L'_R C'_R}\,[rad/s], \\ \omega'_L = 1/\sqrt{L'_L C'_L}\,[rad/s],\end{cases}$ $k = L'_R C'_L + L'_C L'_R\left[(s/rad)^2\right]$ and

$s(\omega) = \begin{cases}-1 & , \omega < \min(\omega_{se}, \omega_{sh}) \\ +1 & , \omega > \max(\omega_{se}, \omega_{sh})\end{cases}$ is called sign function and

$$\begin{cases}\omega_{se} = 1/\sqrt{L'_R C'_L}\,[rad/s], \\ \omega_{sh} = 1/\sqrt{L'_L C'_R}\,[rad/s].\end{cases}$$

For $\omega_{se} < \omega < \omega_{sh}$, the phase constant, β , is an imaginary number, therefore the propagation constant γ, is a real number, which means that the signal on the line is attenuated. Therefore, for $\omega_{se} < \omega < \omega_{sh}$, the circuit behaves as a band-stop filter. If $\omega_{se} = \omega_{sh}$, then there is no stop-band.

The circuit for which $\omega_{se} = \omega_{sh} = \omega_0$ is called a balanced circuit, if not, then it is a unbalanced circuit.

We get $\omega_{se} = \omega_{sh}$ if:

$$L'_R C'_L = L'_L C'_R \qquad (2.10)$$

In this case, we replace the frequencies ω_{se} and ω_{sh} with ω_0 getting the following expression:

$$\omega_0 = \frac{1}{\sqrt{L'_R C'_L}} = \frac{1}{\sqrt{L'_L C'_R}} = \frac{1}{4\sqrt{L'_R C'_L L'_L C'_R}} \tag{2.11}$$

And for balanced circuit, we can analysis from equation (2.9) that, for $\omega < \omega_{se}$ (or ω_0), the line behaves as a LH TL. While for $\omega > \omega_{sh}$ (or ω_0), the line behaves as a RH TL as shown in Fig. 2.5.

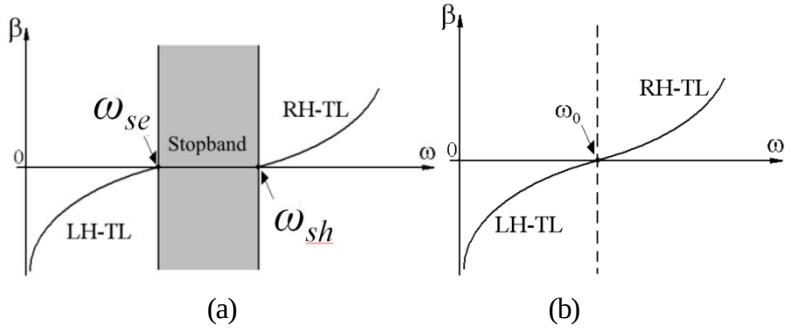

Figure 2.5 Graphic representation of the dispersion equations for CRLH TL, for unbalance case (a) and balanced case (b).

The characteristic impedance for CRLH TL in an unbalanced case is obtained by inserting (2.7) and (2.8) into (2.2):

$$Z_{CRLH} = \sqrt{\frac{L'_L}{C'_L}}\sqrt{\frac{\omega^2 L'_R C'_L - 1}{\omega^2 L'_L C'_R - 1}} \tag{2.12}$$

In balanced case, with the equation (2.10) and (2.12), we can get

$$Z_{CRLH} = \sqrt{\frac{L'_L}{C'_L}} = \sqrt{\frac{L'_R}{C'_R}} \tag{2.13}$$

that means $Z_{CRLH} = Z_{LH} = Z_{RH}$ .With this condition, the impedance matching over a large frequency domain can be easily fulfilled in balanced case.

And in balanced case, using (2.10) in (2.9), we can get:

$$\beta_{CRLH} = \frac{\omega^2 L'_R C'_L - 1}{\sqrt{L'_L C'_L}} = \omega\sqrt{L'_R C'_R} - \frac{1}{\omega\sqrt{L'_L C'_L}} = \beta_{RH} + \beta_{LH} \tag{2.14}$$

As a result, the equivalent circuit for a balanced CRLH-TL can be drawn by connecting in cascade the equivalent circuits for RH-TL and LH-TL.

In this thesis, CRLH TLs are shown to be useful in the design of arbitrary multi-band microwave components. multiband components are beneficial to reduce the number of circuit components in modern wireless communication systems for they can operate at two or more frequency bands simultaneously.

Chapter 3

Multiband Branch Line Coupler (BLC)

This chapter introduces the basic concept and characteristic of BLC.

3.1 Branch Line Coupler (BLC)

Branch line coupler is also called "Quadrature (90º) Hybrid" [7]. BLCs are 3 dB directional couplers with a 90° phase difference in the out puts of the through and coupler arms. The characteristics of BLC are as follows:

- The structure is supposed to be symmetrical.
- Port 1 is matched, no power at port 4.
- -90° phase shift from port 1 to 2; -180° phase shift from port 1 to 3.
- The power is divided into half to port 2 and port 3.

With reference to Fig. 3.1, the basic operation of the branch-line coupler is as follows. With all ports matched, power entering port 1 is evenly divided between ports 2 and 3, with a 90◦ phase shift between these outputs. No power is coupled to port 4 (the isolated port). The scattering matrix has the following form:

$$[S] = \frac{-1}{\sqrt{2}} \begin{bmatrix} 0 & j & 1 & 0 \\ j & 0 & 0 & 1 \\ 1 & 0 & 0 & j \\ 0 & 1 & j & 0 \end{bmatrix} \tag{3.1}$$

Observe that the branch-line hybrid has a high degree of symmetry, as any port can be used as the input port. The output ports will always be on the opposite side of the junction from the input port, and the isolated port will be the remaining port on the same side as the input port. This symmetry is reflected in the scattering matrix, as each row can be obtained as a transposition of the first row.

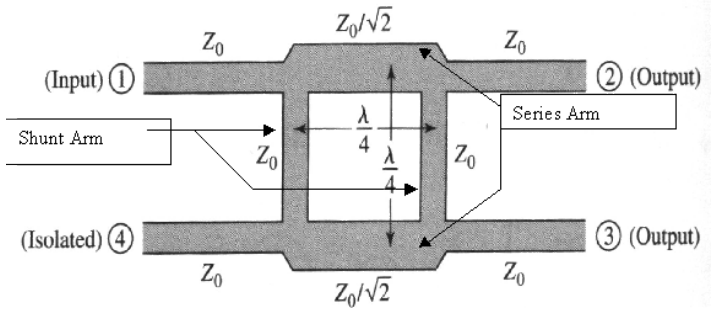

Figure 3.1 Geometry of a branch-line coupler

3.2 Multiband Branch Line Coupler (BLC)

In BLC design, λ/4 length transmission lines with the characteristic impedance 50 Ω and 35.4 Ω are connected together and formed into a rectangle. The λ/4 length conventional transmission lines, which are referred to as right-handed (RH) TLs, only operate at a fundamental frequency f_1 and its odd harmonics [7, 9-10]. The second operating frequency of a conventional BLC is usually the first odd harmonic or $3f_1$. Thus, RH TLs are not practical in dual-band configurations since current wireless standards do not employ

operating frequencies separated by a factor of three. This limitation can be overcome by implementing components consisting of CRLH TLs. The dual-band components realized by CRLH TLs have a first operating frequency at the fundamental frequency f_1, and a variable second operating frequency, which is not necessarily $3f_1$.

.

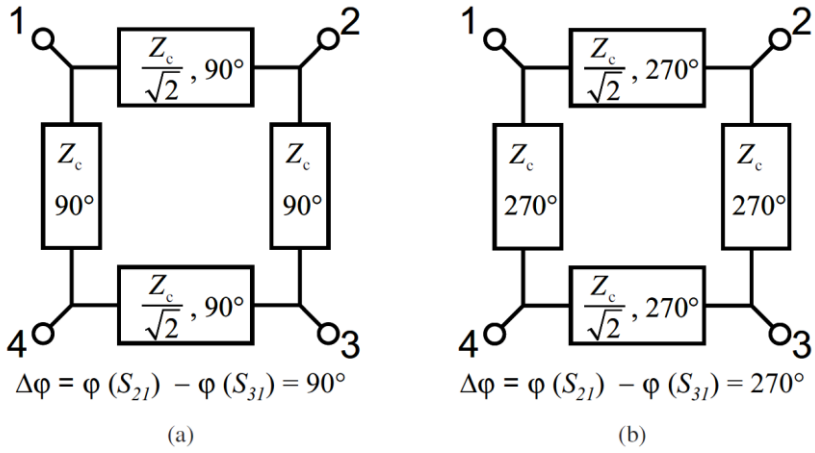

Figure 3.2 Conceptual schematics of the DB BLC: (a) At the first frequency, f_1. (b) At the second frequency, f_2. Z_c represents the characteristic impedance of the input and output lines. From [4]

A dual-band BLC is obtained by replacing the RH TLs in a conventional BLC with CRLH TLs, which have phase responses working at designated frequencies f_1 and f_2. The conceptual schematics of the dual-band BLC are shown in Fig. 3.2. At f_1 , the dual-band BLC works in the same way as the conventional BLC. At f_2 , the phase response of each branch line becomes 270°. From the even–odd-mode analysis of the structure in Fig. 3.2(b) [7], the only difference between two circuits in Fig. 3.2(a) and (b) is the sign of the phase difference between the output signals of ports 2 and 3.

In tri-band BLCs, at the designated 3 bands, the combination may be (a) -(b)- (a), or

(a)-(a)-(b), or others. That depends on the phase responses the designer choose in designing tri-band BLC.

3.3 Size Reduction of BLC (DB BLC example [8])

If the BLC works at the two frequencies of f_1 and f_2, the corresponding phase response pair at the DB should be (-π/2 and -3π/2) or ±π/2.There is an obvious influence on how we chose the pair of phase responses.

If the pair of "π/2, -π/2"is chosen, then

$$\begin{cases} -2\pi f_1 N\sqrt{L_R C_R} + \dfrac{N}{2\pi f_1\sqrt{L_L C_L}} \approx \dfrac{\pi}{2} \\ -2\pi f_2 N\sqrt{L_R C_R} + \dfrac{N}{2\pi f_2\sqrt{L_L C_L}} \approx -\dfrac{\pi}{2} \end{cases} \tag{3.2}$$

Letting $P = 2\pi N\sqrt{L_R C_R}$, the solution of (3.2) can be found as

$$P = \frac{\pi}{2}\frac{1}{f_2 - f_1} \tag{3.3}$$

It is noted that the pair of phase responses in [4] are

$$P' = \frac{\pi}{2}\frac{3f_2 - f_1}{f_2^2 - f_1^2} \tag{3.4}$$

The RH TL part of the BLC is realized with a normal microstrip line. *P* or *P'* can be used

to obtain the proper length of the RH TL part, which determines the overall circuit size of the BLC. As a result, at the same DB frequencies, the length of the RH TL part can change according to *P*.

$$\frac{P}{P'} = \frac{\frac{\pi}{2}\frac{1}{f_2 - f_1}}{\frac{\pi}{2}\frac{3f_2 - f_1}{f_2^2 - f_1^2}} = \frac{f_2 + f_1}{3f_2 - f_1} = \frac{\alpha + 1}{3\alpha - 1} < 1 \tag{3.5}$$

P can be compared to *P′* with $f_2 = \alpha f_1$ and $\alpha > 1$ using (3.5). It is obvious that *P* is always smaller than *P′*. Consequently, the length of TL can be reduced, along with the circuit size. Moreover, another conclusion can be drawn from (3.5), stating that the reduction of circuit size is more obvious if f_2 is further from f_1.

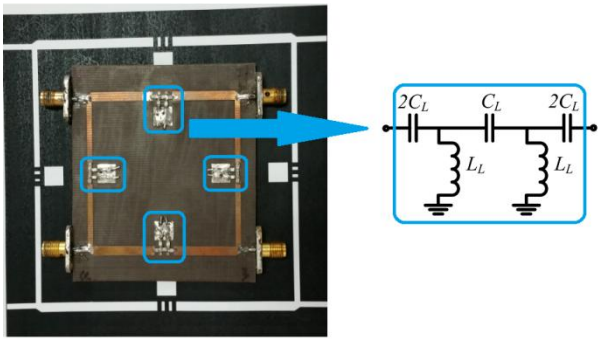

Figure 3.3 Comparison of the circuit size of the proposed DB BLC (fabrication) and the CAD layout designed by [4]

Fig. 3.3 shows the fabricated circuit of the proposed DB BLC and the layout designed by the method in [4] overlapped for the same f_1 and f_2 and substrate. The size of the circuit layout using the previous method is 90.5×93.5 mm^2. It is noted that the size of the proposed DB BLC is 52×56 mm^2, which is only 34.4% of that of the previous method.

This example proves that, by choosing the LH range phase response, the circuit size can be reduced. Because LH TLs provide phase advance as a result the length of RH TL is saved. The same theory can be also applied in tri-band BLC design with the purpose of reducing the circuit size.

Chapter 4

Basic Concepts of CLRH

4.1 Double Lorentz CRLH (DL-CRLH)

The concept of D-CRLH is firstly proposed by Christophe Caloz in 2006 [5]. Fig. 4.1 shows the unit cell model of a D-CRLH transmission line. Its series immittance or impedance is a parallel LC tank and its shunt immittance or admittance is a series LC tank. This configuration is thus the dual of the conventional CRLH.

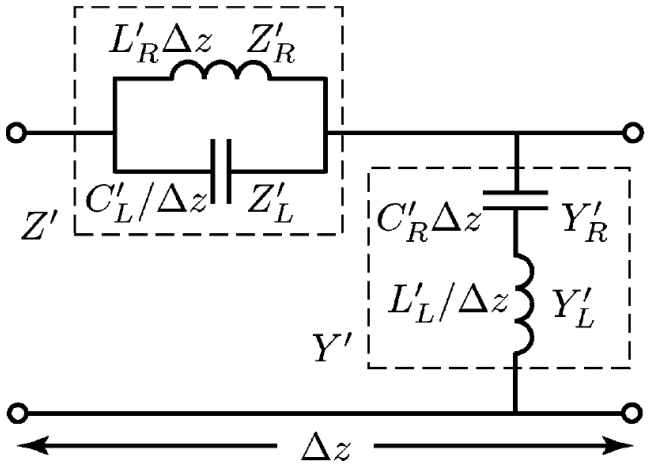

Figure 4.1 The unit cell model of a D-CRLH transmission line

The D-CRLH line has been shown to represent the dual nature of the conventional CRLH and it has interesting complementary characteristics. However, in the practical case, it cannot be exactly realized, because of the existence of the parasitic capacitance and

inductance. In order to apply the D-CRLH TL, parasitic model should be added. That will be what we are going to introduce in the next part.

4.2 Double Lorentz CRLH (DL-CRLH)

Soon after D-CRLH was proposed, the application problem was put on the table. Finally, the double-Lorentz TL metamaterial was proposed [6], and it can exhibit a Lorentz -type dispersion, hence the proposed structure was named double Lorentz. This type of TL presents intrinsic tri-band characteristic and it can be applied in the design of tri-band devices such as TB BPF and TB BLC etc.

Fig. 4.2 shows the incremental circuit model for the DL-CRLH TL (parallel tank circuit with lumped elements L_R, C_L in the series path of the TL and series circuit of L_L, C_R in its shunt path) and of the parasitic series inductance L_P and shunt capacitance C_P). From its structure we can know that a DL CRLH TL is composed of an ideal D CRLH and the parasitic model (RH part).

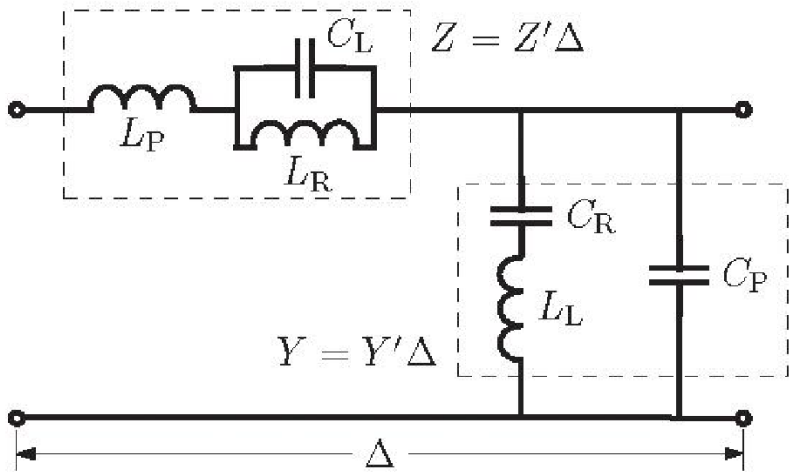

Figure 4.2 The incremental circuit model for the DL-CRLH TL

The DL TL unit cell series impedance Z and shunt admittance Y are given by

$$Z(\omega) = j\omega L_P \frac{\omega^2 - \dfrac{L_R + L_P}{L_R L_P C_L}}{\omega^2{}_L - \dfrac{1}{L_R C_L}} = j\omega L_P \frac{\omega^2 - \omega_0^{se2}}{\omega^2 - \omega_\infty^{se2}} \tag{4.1}$$

$$\text{where } \omega_\infty^{se} = \frac{1}{\sqrt{L_R C_L}}, (\text{series transmission zero})$$

$$\omega_0^{se} = \sqrt{\frac{L_R + L_P}{L_R L_P C_L}} (\text{series transmission pole})$$

$$Y(\omega) = j\omega C_P \frac{\omega^2 - \dfrac{L_R + C_P}{L_L C_R C_P}}{\omega^2 - \dfrac{1}{L_L C_R}} = j\omega L_P \frac{\omega^2 - \omega_0^{sh2}}{\omega^2 - \omega_\infty^{sh2}} \tag{4.2}$$

$$\omega_\infty^{sh} = \frac{1}{\sqrt{L_L C_R}}, (\text{shunt transmission zero})$$

$$\omega_0^{sh} = \sqrt{\frac{C_R + C_P}{L_L C_R C_P}} (\text{shunt transmission pole})$$

The dispersion relation for the homogeneous DL TL, $k_h(\omega) = -j\gamma_h(\omega) = \beta_h(\omega) - j\alpha_h(\omega)$, is obtained from the immittances of Eqs. (4.1) and (4.2) as

$$k_{\mathrm{h}}(\omega)\Delta = \sqrt{-Z(\omega)Y(\omega)}$$

$$= \frac{\omega}{\omega_{\mathrm{p}}}\sqrt{\frac{\omega^2-\omega_0^{se2}}{\omega^2-\omega_\infty^{se2}}\frac{\omega^2-\omega_0^{sh2}}{\omega^2-\omega_\infty^{sh2}}},\ \text{with}\ \omega_{\mathrm{p}} = \frac{1}{\sqrt{L_P C_P}} \tag{4.3}$$

$$Z_h(\omega) = \sqrt{\frac{Z(\omega)}{Y(\omega)}} = \sqrt{\frac{L_P}{C_P}}\sqrt{\frac{\omega^2-\omega_0^{se2}}{\omega^2-\omega_\infty^{se2}}\frac{\omega^2-\omega_\infty^{sh2}}{\omega^2-\omega_0^{sh2}}} \tag{4.4}$$

As the CRLH structure, the DL structure can be balanced, i.e. it can be designed as to exhibit a gap-less transition between the left-handed and right-handed bands. In the case of the DL medium this condition is twofold,

$$\omega_\infty^{se} \equiv \omega_\infty^{sh} \equiv \omega_\infty \text{ and } \omega_0^{se} \equiv \omega_0^{sh} \equiv \omega_0$$

$$\text{namely}\quad \frac{1}{\sqrt{L_R C_L}} = \frac{1}{\sqrt{L_L C_R}} = \omega_\infty, \text{and } \sqrt{\frac{L_R+L_P}{L_R L_P C_L}} = \sqrt{\frac{C_R+C_P}{L_L C_R C_P}} = \omega_0$$

$$\therefore \sqrt{\frac{L_R}{C_R}} = \sqrt{\frac{L_L}{C_L}} = \sqrt{\frac{L_P}{C_P}} = Z_h \quad \text{and} \quad \beta_h(\omega) = \frac{\omega}{\omega_p}\frac{\omega^2-\omega_0^{se2}}{\omega^2-\omega_\infty^{se2}} \tag{4.5}$$

Then the dispersion will be

$$\beta_h(\omega)\Delta = \frac{\omega}{\omega_p}\frac{\omega^2-\omega_0^{se2}}{\omega^2-\omega_\infty^{se2}} = \omega\sqrt{L_PC_P}\,\frac{\omega^2-\frac{L_R+L_P}{L_RL_PC_L}}{\omega^2-\frac{1}{L_RC_L}}$$

$$= \omega\sqrt{L_PC_P}\,\frac{\omega^2L_RC_L-\frac{L_R+L_P}{L_P}}{\omega^2L_RC_L-1} = \omega\sqrt{L_PC_P}\,\frac{\omega^2L_RC_L-1-\frac{L_R}{L_P}}{\omega^2L_RC_L-1}$$

$$= \omega\sqrt{L_PC_P}\left(1-\frac{\frac{L_R}{L_P}}{\omega^2L_RC_L-1}\right) = \omega\sqrt{L_PC_P}+\sqrt{\frac{C_P}{L_P}}\,\frac{\omega L_R}{1-\omega^2L_RC_L}$$

$$\omega\sqrt{L_PC_P}+\sqrt{\frac{C_P}{L_P}}\,\frac{\omega L_R}{1-\omega^2L_RC_L} = \omega_1Z_0C_P+\frac{1}{Z_0}\,\frac{\omega L_R}{1-\omega^2L_RC_L} = -\varphi$$

$$\Rightarrow \omega Z_0^2C_P+\frac{\omega L_R}{1-\omega^2L_RC_L} = -\varphi Z_0 \tag{4.6}$$

If phase responses are "ϕ_1,ϕ_2,ϕ_3" at ω_1, ω_2 and ω_3,

$$\begin{cases} \omega_1Z_0^2C_P+\dfrac{\omega_1L_R}{1-\omega_1^2L_RC_L} = -\phi_1Z_0 \\ \omega_2Z_0^2C_P+\dfrac{\omega_2L_R}{1-\omega_2^2L_RC_L} = -\phi_2Z_0 \\ \omega_3Z_0^2C_P+\dfrac{\omega_3L_R}{1-\omega_3^2L_RC_L} = -\phi_3Z_0 \end{cases} \tag{4.7}$$

With the characteristic impedance relation $Z_0=\sqrt{\frac{L_p}{C_p}}=\sqrt{\frac{L_R}{C_R}}=\sqrt{\frac{L_L}{C_L}}$, all the lumped element values can be found.

4.3 The Phase response of DL-CRLH

We can know there are many options in choosing the group of phase responses at the three bands. Since our target is to realize λ/4 length TL using DL CRLH so that it can provide tri-band characteristic, the overall phase response of a λ/4 length should be -π/2 or -3π/2 (i.e. π/2). If the unit number *N* is chosen to be 2, then the phase of one unit should thus be -π/4 or -3π/4 (i.e. π/4).

A tri-band BLC was proposed by Hanseung Lee in the year of 2008 [11], where the phase responses at the 3 chosen frequency bands were "-π/4, -π/4, -3π/4 ", respectively. The TB BLC can work at f_1 = 0.195 GHz, f_2 = 0.67 GHz and f_3 = 1.465 GHz, which are selected for mobile TV services [12]. The designed TB BLC had acceptable performance at 3 frequency bands. However, the circuit had a bulky size of 89.6×93.1 mm^2, using the substrate Ro4350 with the dielectric constant 3.48 and a thickness of 0.768 mm.

For multiband devices, circuit size is very important in that the purpose of using multiband circuit is to save more space for the system. If the circuit size of the multiband device can be reduced more, then this effect can be optimized. In CRLH dual band BLC's design, a solution was proposed to reduce the circuit size. That is to choose another pair of phase responses where the positive phase response is included. The size of the proposed DB BLC is significantly compact, at 34.4% of the previous DB BLC when they are both designed using DL CRLH TLs for the same DB frequencies.

When the phase responses were "-π/4, -π/4, -3π/4 " at f_1 = 0.195 GHz, f_2 = 0.67 GHz and f_3 = 1.465 GHz. The solution of equation (4.7) can be found as:

$$L_P = 13.4850[\text{nH}] \quad C_P = 5.3940[\text{pF}]$$
$$L_L = 45.3801[\text{nH}] \quad C_L = 18.1520[\text{pF}]$$
$$L_R = 12.3289[\text{nH}] \quad C_R = 4.9316[\text{pF}]$$

In order to observe the characteristic of DL CRLH, a unit model is built using above values in ADS.

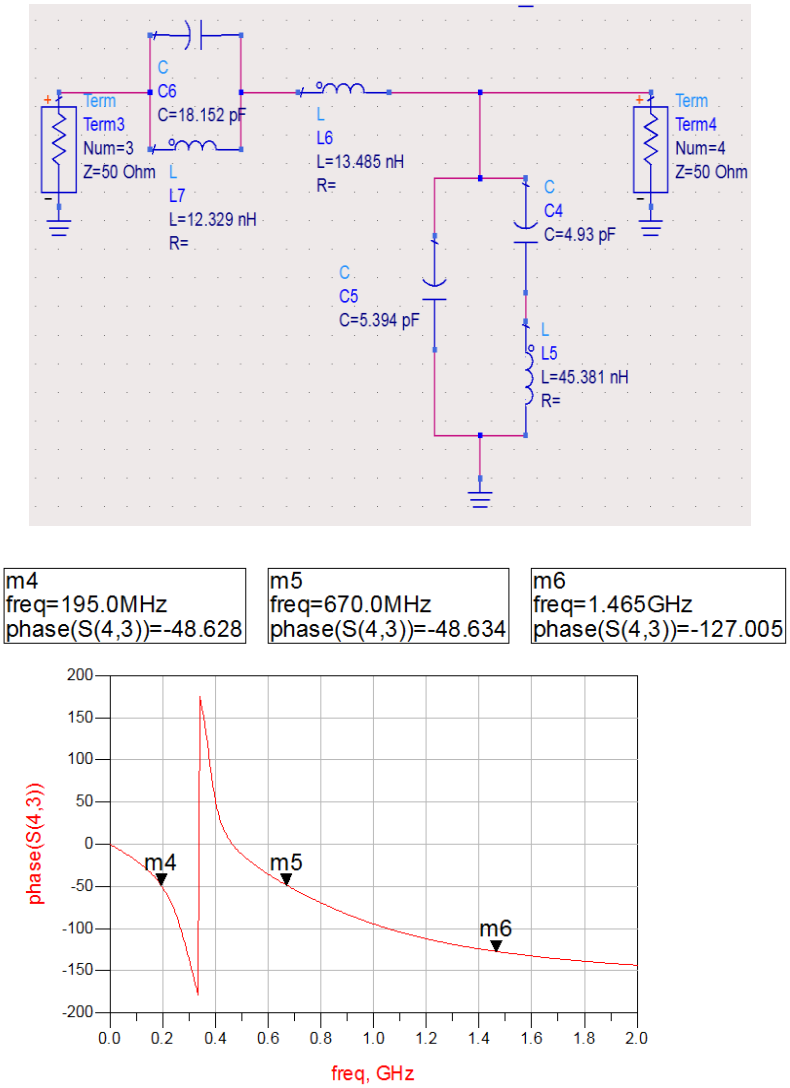

Figure 4.3 ADS simulation of DL CRLH unit cell

From the phase response of the DL-CRLH unit, we can see that at low frequencies, the phase is negative (phase lag) because both the parasitic part and D-CRLH behave as RH TL. As the frequency increases, resonance happens and DL-CRLH unit begins to act as LH TL producing positive phase response, which means phase advance. And when the frequency keeps going high, the parasitic (RH) part becomes dominated in phase and it goes back to negative again. As we know, the phases should have been -45°, -45° and -125°, the slight difference happens here because we use the lumped elements in this structure. As a result, the circuit does not satisfy the homogeneous condition where $\Delta z << \lambda/4$. The error can be reduced when more units are cascaded.

For the TB BLC can work at f_1= 0.195 GHz, f_2= 0.67 GHz and f_3 = 1.465 GHz, if other pairs of phase responses are chosen to reduce the circuit size, they should match these conditions according to the phase characteristic of DL-CRLH

1) ϕ_1 should be negative (f_1 is low frequency, parasitic part and D-CRLH behave as RH TL.)

2) ϕ_3 should be negative (f_3 is high frequency, parasitic (RH) part is dominated)

If the chosen phase group does not agree to these 2 condition, there is no positive solution for all L and C values (some will be negative).

As a result, there are still many options for TB BLC design. All possible solutions are concluded as Table 1.

TABLE 1 POSSIBLE PHASE RESPONSES OF DL-CRLH UNIT AND CORRESPONDING LUMPED ELEMENT VALUES

Phase responses ϕ_1, ϕ_2, ϕ_3	L_P (nH)	C_P (pF)	L_L (nH)	C_L (pF)	L_R (nH)	C_R (pF)
-π/4 -π/4 -3π/4	13.4850	5.3940	45.3801	18.1520	12.3289	4.9316
-π/4 π/4 -π/4	6.3131	2.5253	15.8417	6.3367	20.6760	8.2704
-π/4 π/4 -3π/4	15.0051	6.0021	15.3754	6.1502	14.7282	5.8913
-3π/4 -π/4 -3π/4	13.5974	5.4390	37.9697	15.1879	28.6430	11.4572
-3π/4 π/4 -π/4	7.0462	2.8185	11.1420	4.4568	55.8260	22.3304
-3π/4 π/4 -3π/4	16.8268	6.7307	7.8356	3.1342	57.7666	23.1066
-π/4 3π/4 -π/4	7.4636	2.9854	10.6162	4.2465	21.2561	8.5024
-π/4 3π/4 -3π/4	15.5175	6.2070	12.8646	5.1459	14.6612	5.8645
-3π/4 3π/4 -π/4	9.7031	3.8812	5.8722	2.3489	66.2542	26.5017
-3π/4 3π/4 -3π/4	18.9394	7.5758	5.2806	2.1122	62.0280	24.8112

Figure 4.4 exhibits a schematic of the DL CRLH TL. The D CRLH section of DL CRLH TL consists of two T-type unit cells with parallel resonant structures in impedance part and series resonant structures in admittance part. These resonant structures are implemented by SMT chip components [13]. The RH section of DL CRLH TL is accomplished by two microstrip lines on each side of the LH section.

In this case, total phase shift ϕ is divided into the D-CRLH TL phase shift ϕ_{D} and RH TL phase shift ϕ_{RH}. The RH section implemented by microstrip line is designed by determining the characteristic impedance Z_0 and the RH phase delay ϕ_{RH}, provided in (4.7) and (4.8), respectively.

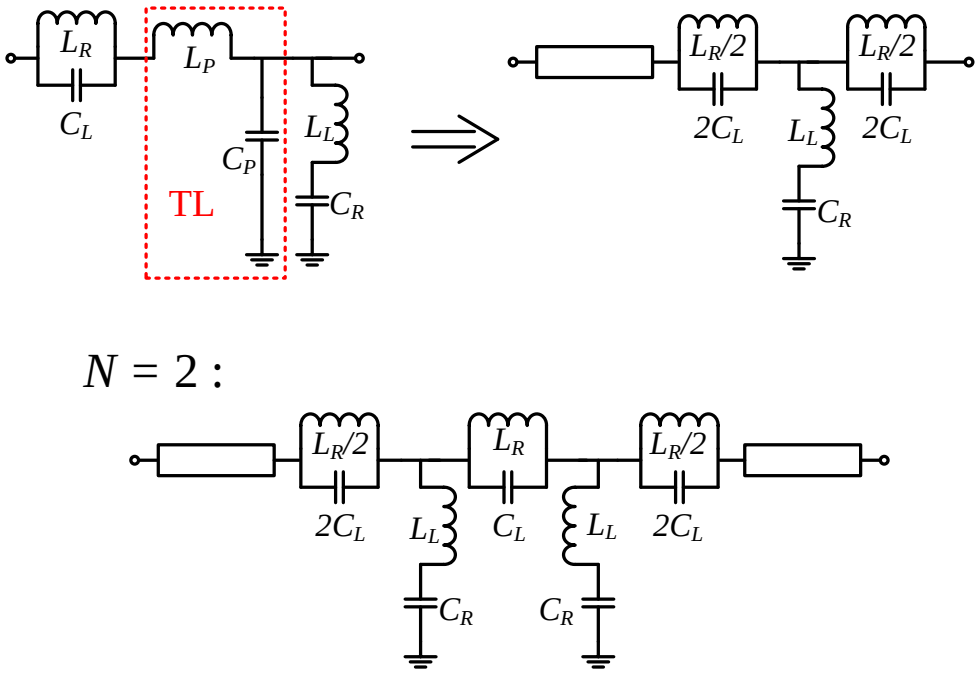

Figure 4.4 DL CLRH TL with the unit number $N = 2$

$$Z_0 = \sqrt{\frac{L_P}{C_P}} \tag{4.7}$$

$$\phi_{RH} = -N\omega_1\sqrt{L_P C_P} \tag{4.8}$$

From (4.8), we know that the electrical length of the RH part is decided by the values of $L_P \times C_P$. And the overall length of DR CRLH TL is also dependent on the RH part. As a consequence, the circuit size of a TB BLC designed by DR CRLH TL depends on the calculated values of $L_P \times C_P$. In TABLE 1, we can easily find that when the phase responses are chosen to be"-π/4, π/4, -π/4 ", the calculated values of $L_P \times C_P$ is the smallest. That means, "-π/4, π/4, -π/4 " is the best solution to reduce the circuit size of TB BLC.

4.4 Compact TB BLC Design:

Since the phase responses of "-π/4, π/4, -π/4 " has been chosen, the lumped element values are listed as below:

$$L_P = 6.3131[\text{nH}] \quad C_P = 2.5253[\text{pF}]$$
$$L_L = 15.8417[\text{nH}] \quad C_L = 6.3367[\text{pF}]$$
$$L_R = 20.6760[\text{nH}] \quad C_R = 8.2704[\text{pF}]$$

In practical, RH part is realized by conventional TL and the physical length can be calculated by:

$$\theta = -\phi_{RH} = N\omega_1\sqrt{L_P C_P} = 1\times\omega_1\times\sqrt{L_P C_P} = 8.8631[\text{deg}]$$

Then, we can simulate the DR-CRLH unit cell using ADS 2009. The layout and si mulation result are shown in Fig. 4.5.

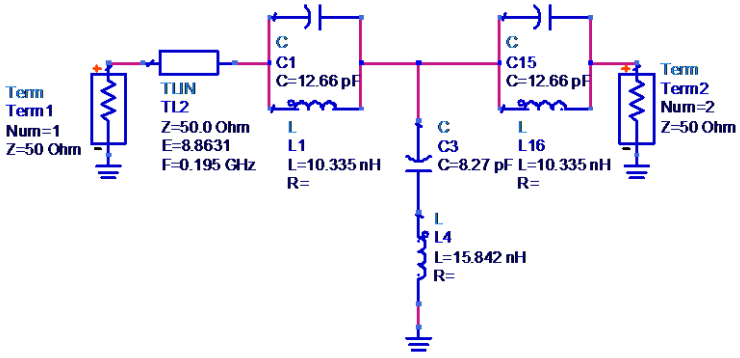

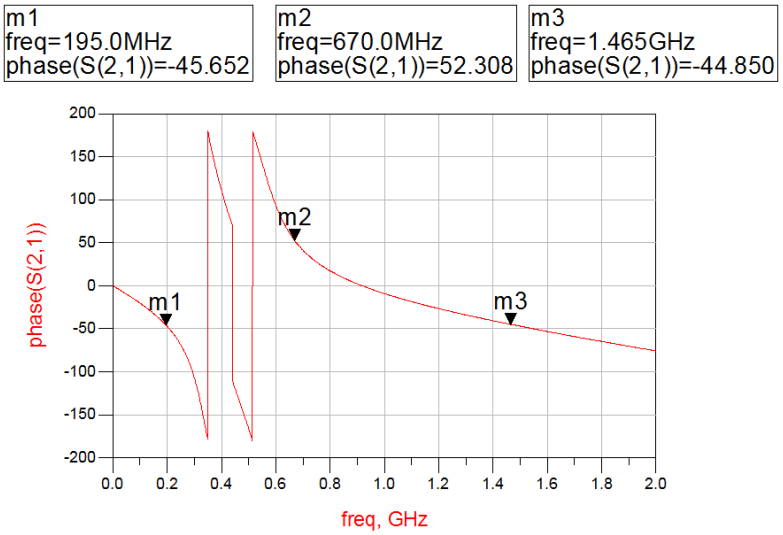

Figure 4.5 ADS simulation of DL CRLH unit realized with RH TL and LEs

In ADS simulation result, we can see the phase responses are not correct, especially at 2nd frequency band. It should have been 45°, however we get 52.308° from simulation. This error happens because our calculation was performed under the assumption of homogenous model of DL CRLH TL. And specially, in the second band, the DL CRLH behave as LH TL. However, in our design, lumped elements are used to realize LH TL, which can produce much error. The reasons are as follows:

1) This is only 1 unit, homogenous condition ($\Delta z < \frac{\lambda_g}{4}$) is not satisfied.

2) The lumped element model is different from naturally formed material.

The second reason is dominated to this problem. However, we can do nothing to it since natural LH material does not exist. And any kind of artificial LH material produces some error more or less.

In order to figure out the real phase response of DL-CRLH TL. The unit cell is thus to be analyzed by ABCD matrix.

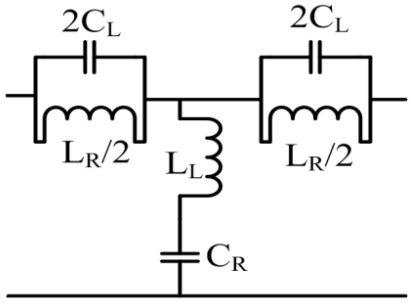

Figure 4.6 D-CRLH unit cell

$$\begin{bmatrix} A & B \\ C & D \end{bmatrix} = \begin{bmatrix} 1 & \dfrac{j\omega L_R}{2-2\omega^2 L_R C_L} \\ 0 & 1 \end{bmatrix} \begin{bmatrix} 1 & 0 \\ \dfrac{j\omega C_R}{1-\omega^2 L_L C_R} & 1 \end{bmatrix} \begin{bmatrix} 1 & \dfrac{j\omega L_R}{2-2\omega^2 L_R C_L} \\ 0 & 1 \end{bmatrix}$$

$$= \begin{bmatrix} 1-\dfrac{\omega^2 L_R C_R}{\left(2-2\omega^2 L_R C_L\right)\left(1-\omega^2 L_L C_R\right)} & \dfrac{2j\omega L_R}{2-2\omega^2 L_R C_L} - \dfrac{j\omega^3 L_R^2 C_R}{\left(2-2\omega^2 L_R C_L\right)^2\left(1-\omega^2 L_L C_R\right)} \\ \dfrac{j\omega C_R}{1-\omega^2 L_L C_R} & 1-\dfrac{\omega^2 L_R C_R}{\left(2-2\omega^2 L_R C_L\right)\left(1-\omega^2 L_L C_R\right)} \end{bmatrix}$$

(4.9)

$$S_{21} = \frac{2}{A + B/Z_0 + CZ_0 + D}$$

$$= \frac{2}{2 - \dfrac{2\omega^2 L_R C_R}{\left(2-2\omega^2 L_R C_L\right)\left(1-\omega^2 L_L C_R\right)} + \dfrac{2j\omega L_R}{Z_0\left(2-2\omega^2 L_R C_L\right)} - \dfrac{\omega^3 jL_R^2 C_R}{Z_0\left(2-2\omega^2 L_R C_L\right)^2\left(1-\omega^2 L_L C_R\right)} + \dfrac{j\omega Z_0 C_R}{1-\omega^2 L_L C_R}}$$

$$\phi = -\arctan \frac{\dfrac{2\omega L_R}{Z_0\left(2-2\omega^2 L_R C_L\right)} - \dfrac{\omega^3 L_R^2 C_R}{Z_0\left(2-2\omega^2 L_R C_L\right)^2\left(1-\omega^2 L_L C_R\right)} + \dfrac{\omega Z_0 C_R}{1-\omega^2 L_L C_R}}{2 - \dfrac{2\omega^2 L_R C_R}{\left(2-2\omega^2 L_R C_L\right)\left(1-\omega^2 L_L C_R\right)}}$$

$$= -\arctan \frac{2\omega L_R\left(1-\omega^2 L_L C_R\right)\left(2-2\omega^2 L_R C_L\right) - \omega^3 L_R^2 C_R + \omega Z_0^2 C_R\left(2-2\omega^2 L_R C_L\right)^2}{2Z_0\left(2-2\omega^2 L_R C_L\right)^2\left(1-\omega^2 L_L C_R\right) - 2Z_0\omega^2 L_R C_R\left(2-2\omega^2 L_R C_L\right)} \tag{4.10}$$

As a result, the overall phase response of a DL-CRLH TL unit should be

$$\phi_{DL-CRLH} = -\omega\sqrt{L_P C_P} - \arctan \frac{2\omega L_R\left(1-\omega^2 L_L C_R\right)\left(2-2\omega^2 L_R C_L\right) - \omega^3 L_R^2 C_R + \omega Z_0^2 C_R\left(2-2\omega^2 L_R C_L\right)^2}{2Z_0\left(2-2\omega^2 L_R C_L\right)^2\left(1-\omega^2 L_L C_R\right) - 2Z_0\omega^2 L_R C_R\left(2-2\omega^2 L_R C_L\right)} \tag{4.11}$$

This is the practical phase response of the unit cell with lumped D-CRLH termi nated to a transmission line, which is RH part. Since it is derived, this method is also possible theoretically.

$$\phi_{DL-CRLH}\left(\omega_1\right) = \phi_1, \phi_{DL-CRLH}\left(\omega_2\right) = \phi_2, \phi_{DL-CRLH}\left(\omega_3\right) = \phi_3$$

However, these equations are too difficult to solve even with the help of computer programming, while they can be helpful to check and optimize the phase value.

In order to compare how much error produced in the practical case. The phase expression of equation (4.6) (phase of homogenous model) and (4.11) (practical phase) is plotted as Fig 4.7.

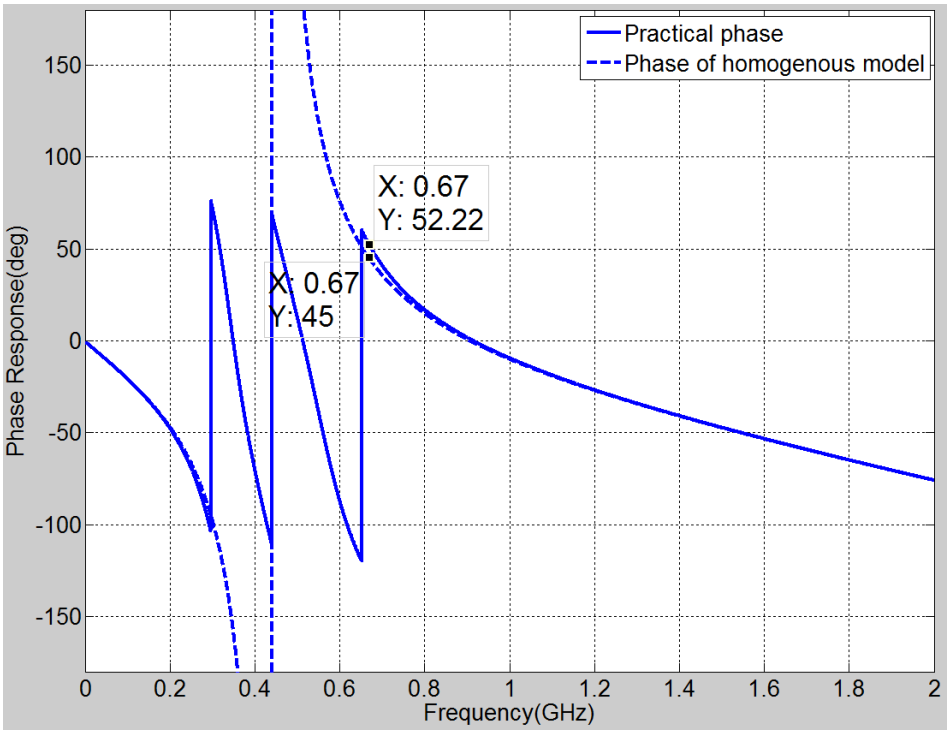

Figure 4.7 The phase plot of homogenous model and practical case

From Fig. 4.7 we can observe that in RH phase range, namely phase < 0, phase of homogenous model and practical phase are almost same. However, in LH phase range, there is a difference that cannot be ignored. That is to say, the homogenous model analysis method has the problem when positive phases (LH range) are chosen.

In order to solve this problem, the phase in the second band should be optimized so that it can be fit for the accurate phase. From Fig. 4.7 we can figure out that when the phase is 45° in the practical case , then, in homogenous model, the phase is not 45° but other value near 45°. Let us name this phase $\phi_{\omega 2}$.

Until now, the problem comes to how to find $\phi_{\omega 2}$, where the virtual phase is 45° at ω_2. Because $\phi_{\omega 2}$ is near to 45°, we can set the range from 35°~55° and set the step by 1°. After

we find a smaller range of $\phi_{\omega 2}$, the step can be reduced to 0.1° in that range to get the accurate $\phi_{\omega 2}$. This process can be realized with the help of loop program in MATLAB .

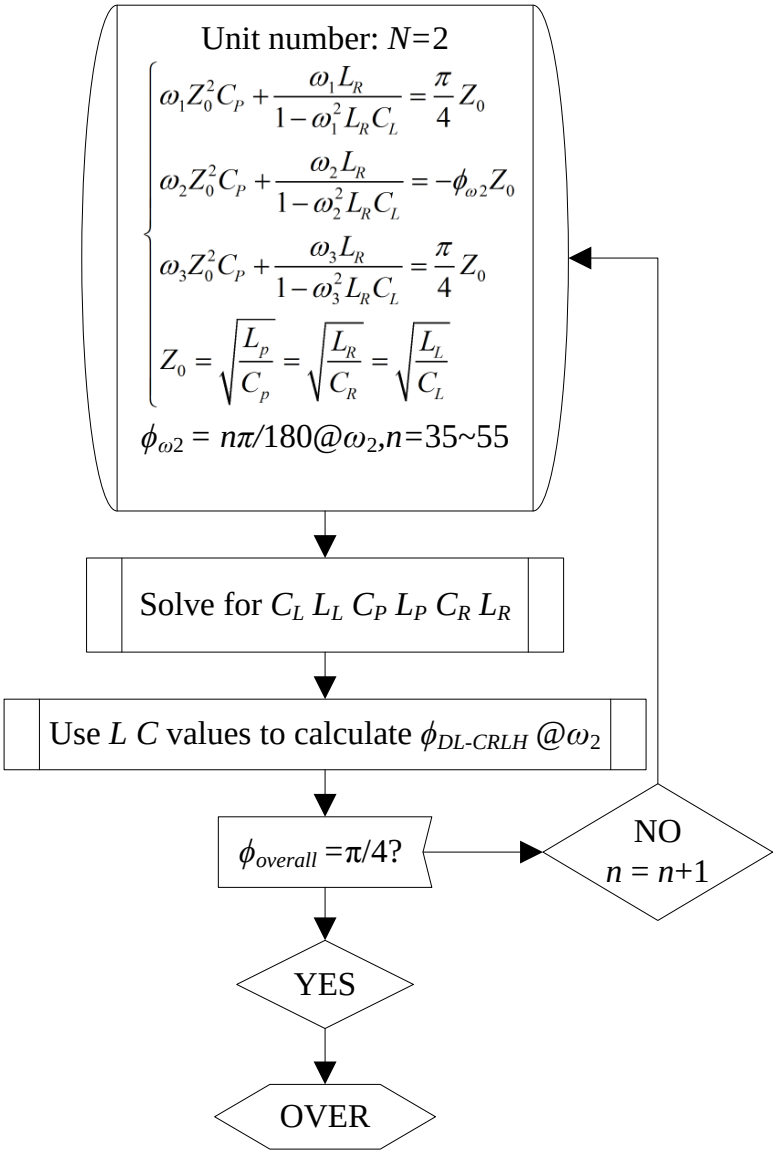

Figure 4.8 The flowing chart of loop program to optimize the phase characteristic

TABLE 2 TWO STEPS TO FIND $\phi_{\text{DL CRLH}}$

STEP1				STEP2	
ϕ_2	$\phi_{\text{DL CRLH}}$	ϕ_2	$\phi_{\text{DL CRLH}}$	ϕ_2	$\phi_{\text{DL CRLH}}$
35	0.6868	46	0.9344	39.1	0.7770
36	0.7086	47	0.9578	39.2	0.7792
37	0.7305	48	0.9812	39.3	0.7815
38	0.7525	49	1.0048	39.4	0.7837
39	0.7748	50	1.0286	39.5	0.7854
40	0.7971	51	-2.0892	39.6	0.7882
41	0.8197	52	-2.0653	39.7	0.7904
42	0.8423	53	-2.0413	39.8	0.7926
43	0.8651	54	-2.0172	39.9	0.7949
44	0.8881	55	-1.9930	40.0	0.7971

Table 2 shows the calculating process of $\phi_{\omega 2}$. The purpose phase is $\pi/4$ (0.7854). In the 1st step, we set the range of 35°~55 °, and $\phi_{\omega 2}$ is found between 39 °~ 40 °. As a result. In the 2nd step, we start to search where $\phi_{\omega 2}$ is exactly located. By this means, $\phi_{\omega 2}$ is found to be 39.5°, where it reaches to the purpose phase $\pi/4$ (0.7854). After $\phi_{\omega 2}$ is found, we can use it to calculate lumped element values.

$$\begin{cases} \omega_1 Z_0^2 C_P' + \dfrac{\omega_1 L_R'}{1-\omega_1^2 L_R' C_L'} = \dfrac{\pi}{4} Z_0 \\ \omega_2 Z_0^2 C_P' + \dfrac{\omega_2 L_R'}{1-\omega_2^2 L_R' C_L'} = -\dfrac{39.5\pi}{180} Z_0 \\ \omega_3 Z_0^2 C_P' + \dfrac{\omega_3 L_R'}{1-\omega_3^2 L_R' C_L'} = \dfrac{\pi}{4} Z_0 \\ Z_0 = \sqrt{\dfrac{L_p'}{C_p'}} = \sqrt{\dfrac{L_R'}{C_R'}} = \sqrt{\dfrac{L_L'}{C_L'}} \end{cases} \tag{4.12}$$

Equation (4.12) can be solved as:

$$L_P = 6.2029[\text{nH}] \quad C_P = 2.4811[\text{pF}]$$
$$L_L = 16.6723[\text{nH}] \quad C_L = 6.6689[\text{pF}]$$
$$L_R = 20.5346[\text{nH}] \quad C_R = 8.2138[\text{pF}]$$

Here, the RH part is realized by conventional TL and the physical length can be calculated by:

$$\theta = -\phi_{RH} = N\omega_1\sqrt{L_P C_P} = 1\times\omega_1\times\sqrt{L_P C_P} = 8.7077[\text{deg}]$$

Then, we can try these new parameters in ADS simulation for DL CRLH unit to check the performance of the phase response.

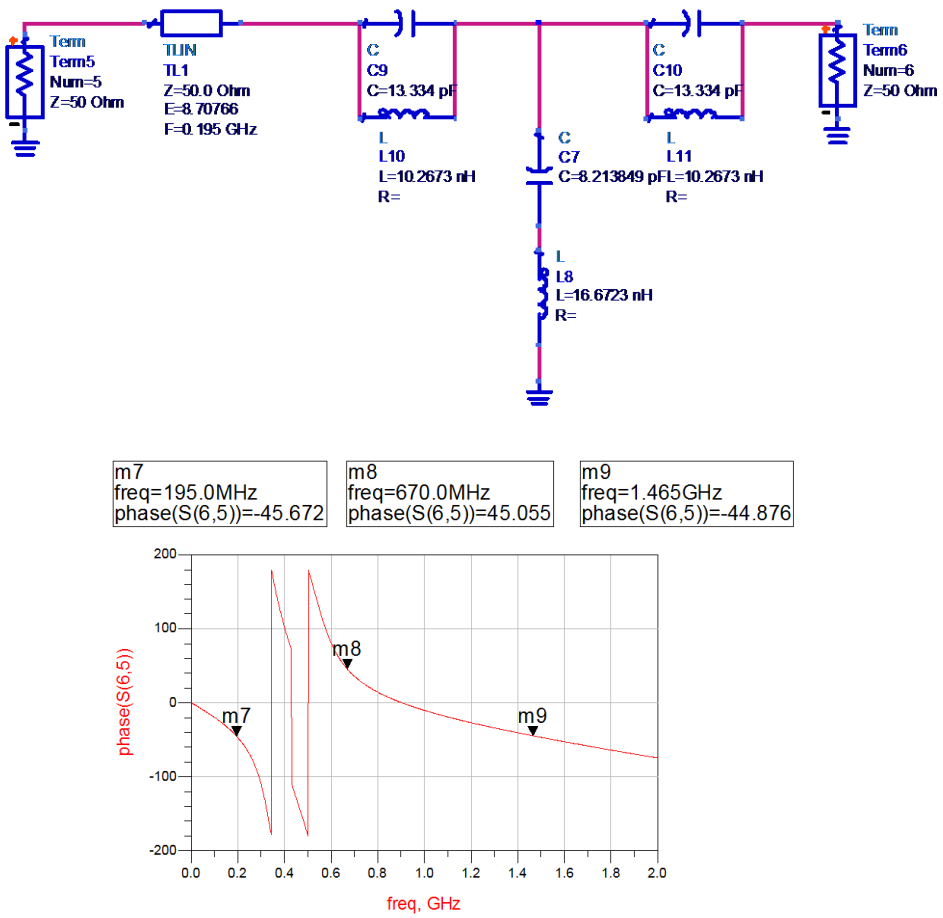

Figure 4.9 ADS simulation with optimized phase of DL CRLH

From the simulation result we can see our design parameters can satisfy our design purpose. This proves that our design method is available in optimizing the phase characteristic in the LH phase range. Using this unit, we can design tri-band λ/4 DL CRLH TL and TB BLC.

Before BLC design, we first design a λ/4 length DL CRLH open-circuit stub to check the tri-band characteristic. The λ/4 open- and short- circuit stubs are widely used as harmonic

terminations. A λ/4 DL CRLH open-circuit stub terminates signals at frequencies of f_1, f_2, f_3 and other higher frequencies. Higher frequencies are not integer multiples of f_1 because of the nonlinear phase response of the LH TL. Therefore, the λ/4 DL CRLH TL provides more flexibility for terminating harmonics.

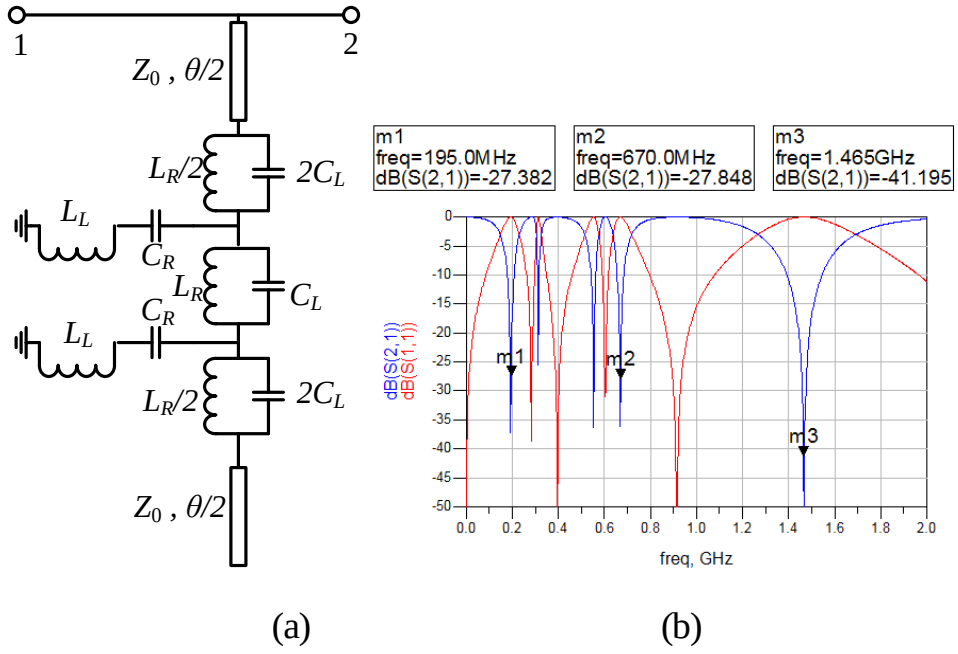

Figure 4.10 ADS simulation of λ/4 DL CRLH open-circuit stub:

(a)Layout ; (b)*S*-parameters

A tri-band BLC is obtained by replacing the RH TLs in a conventional BLC with DL CRLH TLs, which work at designated frequencies. In this thesis, our design substrate is teflon Rogers RT/duroid 5880 with the dielectric constant (ε_r) of 2.2 and thickness of 31 mils. ADS simulation was performed as Fig. 4.11 shows. In practice, we selected the available lumped capacitor values in laboratory that slightly differ from the calculated values.

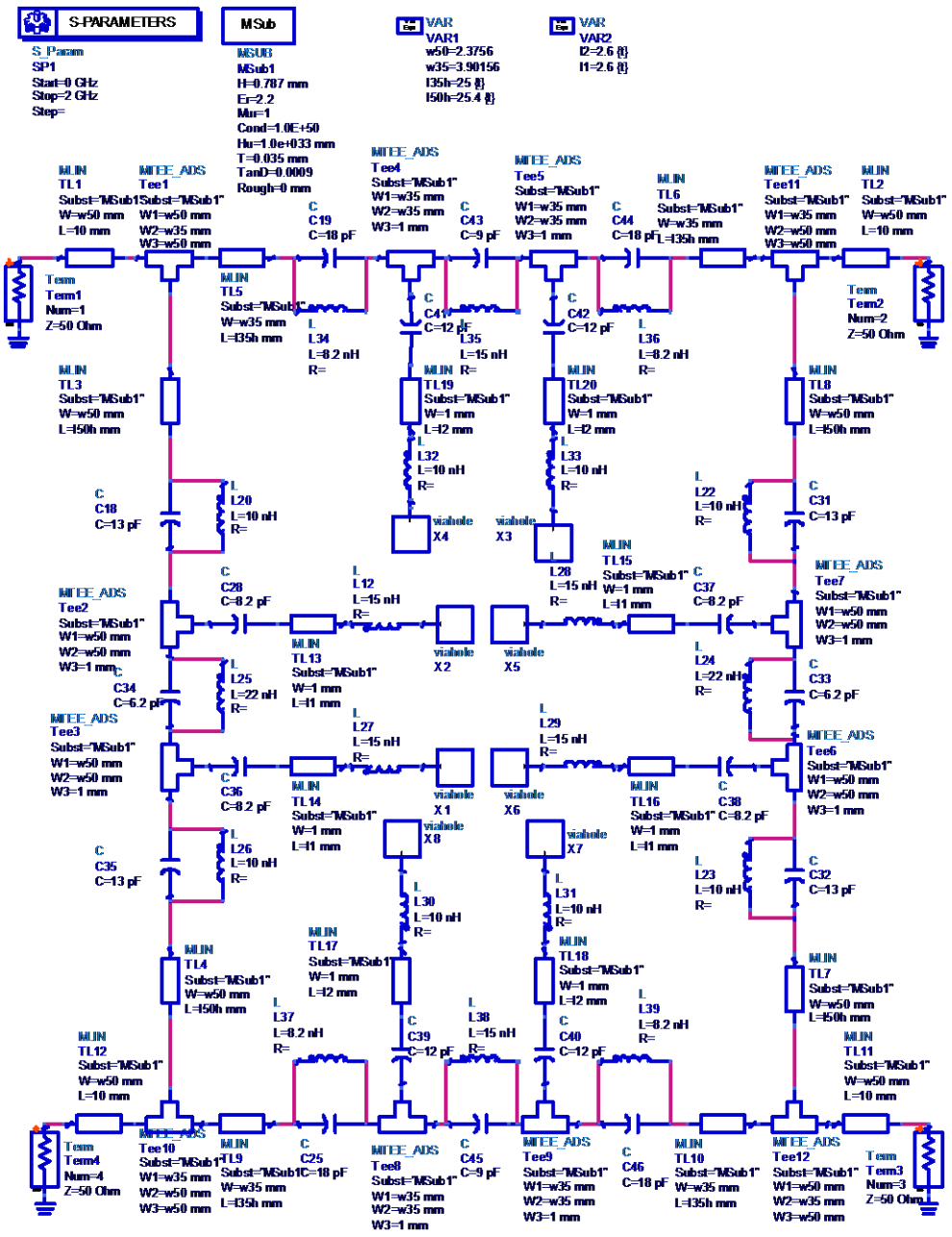

Figure 4.11 ADS layout of DL CRLH TB BLC

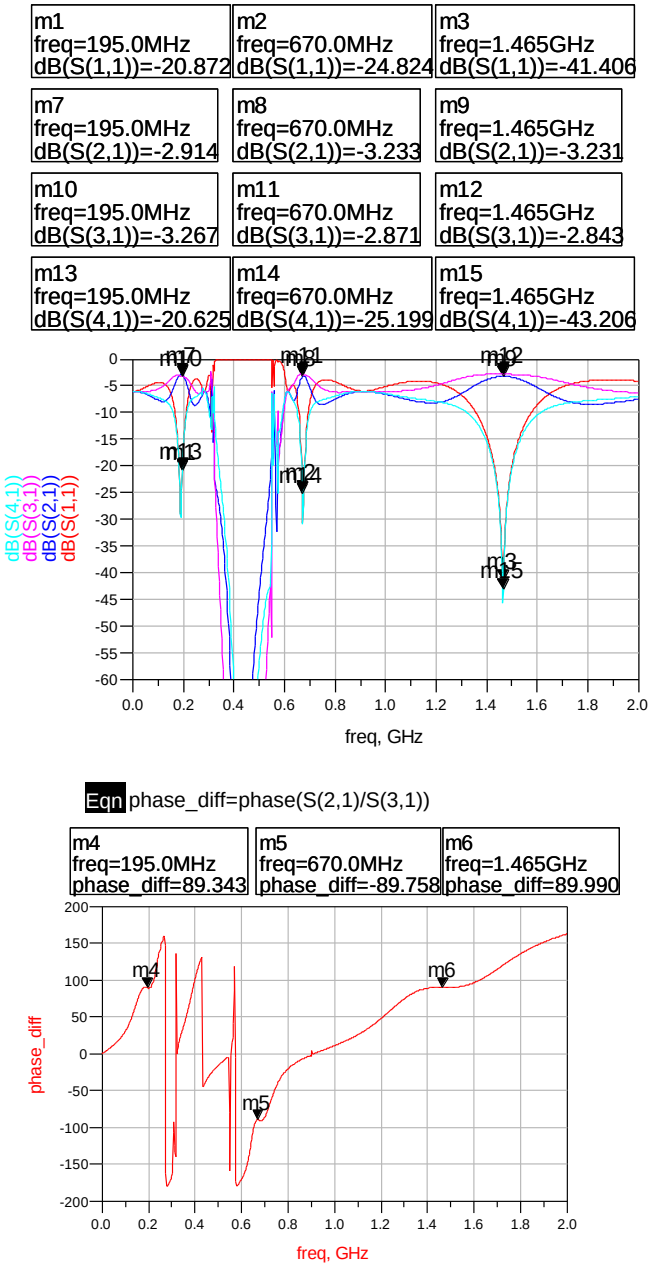

Figure 4.12 ADS simulation results of *S*-parameters and phase difference

The EM simulation was performed by high frequency structure simulator (HFSS) v13 from Ansys. The layout of EM simulation is shown in Fig. 4.13 with the dimension specifications.

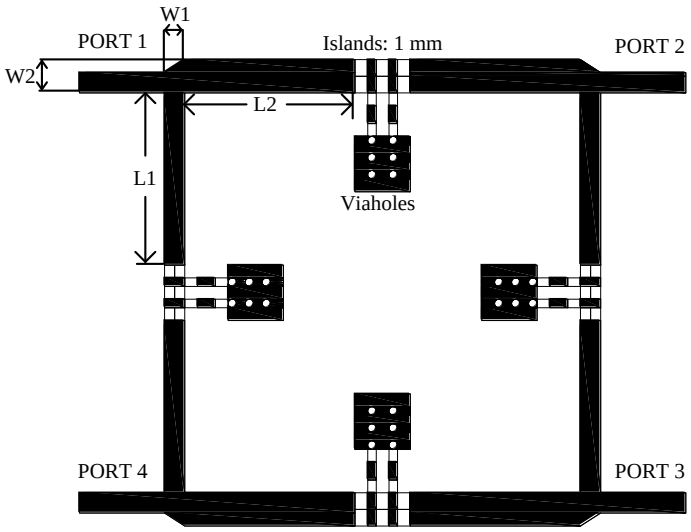

L1	20.2	mm
W1	2.375	mm
L2	20	mm
W2	3.9	mm

Figure 4.13 EM simulation layout

The simulated and measured *S*-parameters of the fabricated TB BLC are compared in Fig. 4.14 and Fig. 4.15, respectively, and are summarized in Table 2 and Table 3, respectively. We can see the simulation and measurement results agree well to each other. In both simulation and measurement, it is shown that the operation at tri-frequencies has been well attained. Fig. 4.15 shows the simulated and measured phase differences between output ports. The expected phase performances are seen clearly at all 3 frequencies. The

proposed design principle is clearly verified.

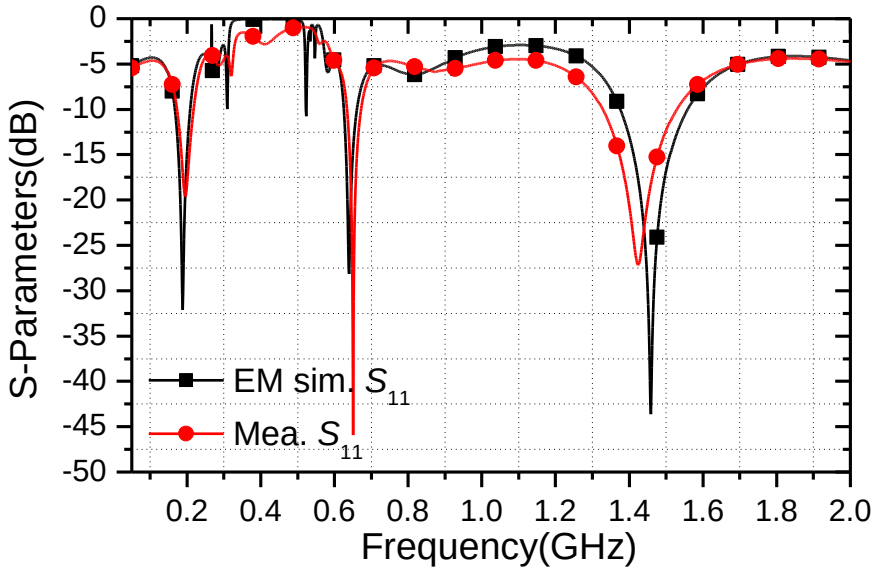

(a) S_{11} of EM simulation and measurement

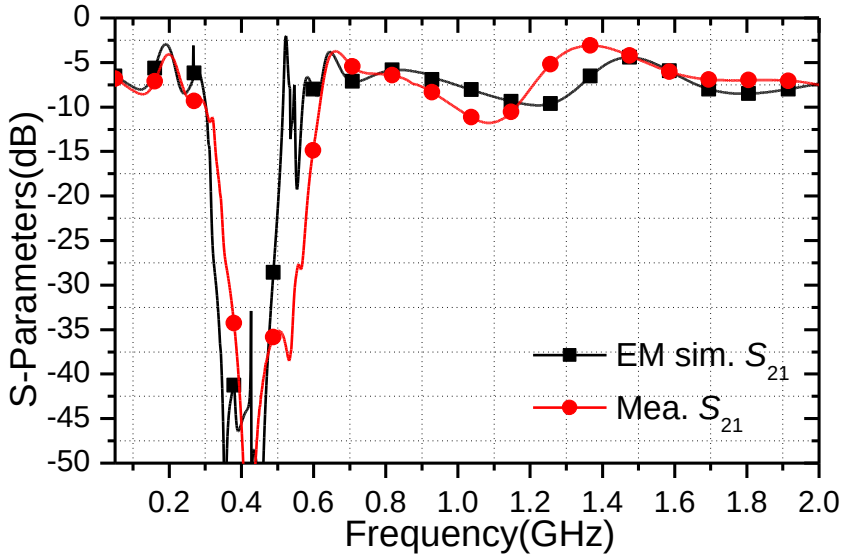

(b) S_{21} of EM simulation and measurement

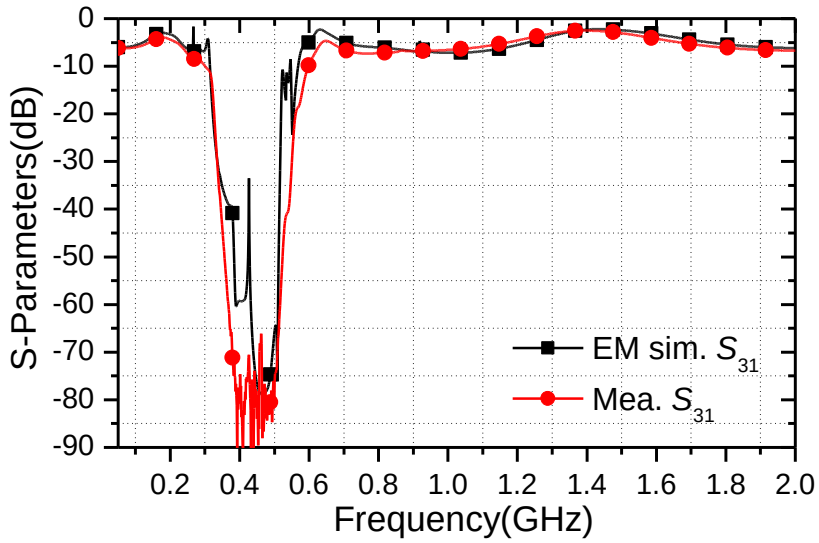

(c) S_{31} of EM simulation and measurement

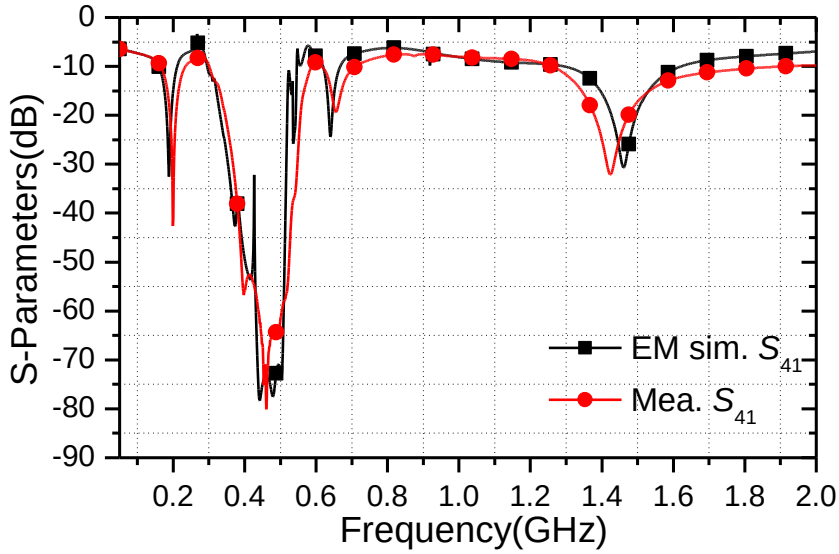

(d) S_{41} of EM simulation and measurement

Figure 4.14 The comparison between EM simulation and measurement

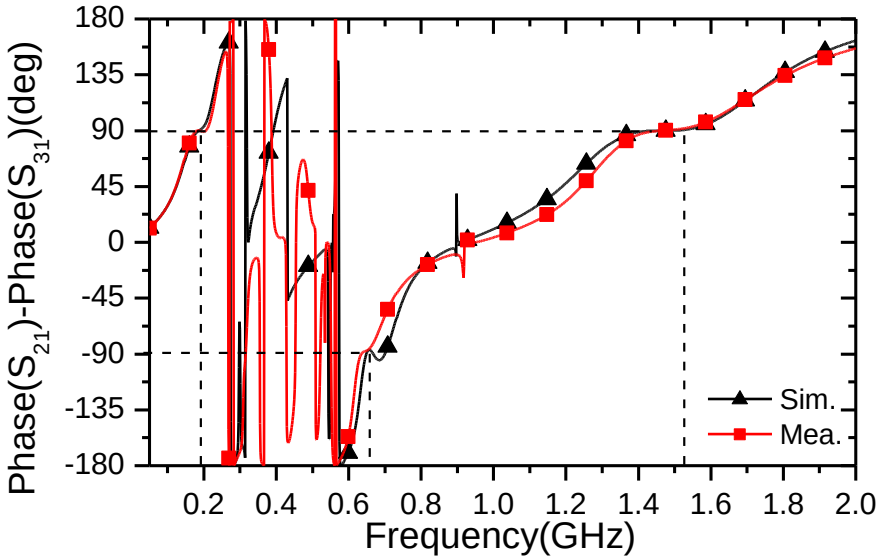

Figure 4.15 The phase difference performance of EM simulation and measurement.

TABLE 3. EM SIMULATION OF PROPOSED BLC.

	Simulation		
	f_1 = 0.190 GHz	f_2 = 0.645 GHz	1.465GHz
Return loss (S_{11})	27.03 dB	20.2 dB	32.63 dB
Isolation (S_{41})	26.48dB	19.4 dB	-30.2 dB
Output 1 (S_{21})	-2.95 dB	-3.8 dB	-4.4 dB
Output 2 (S_{31})	-3.16 dB	-2.7 dB	-3.3 dB
Phase difference	-90.1°	88°	-90

TABLE 4. MEASUREMENT RESULT OF PROPOSED BLC.

	Measurement		
	f_1 = 0.195 GHz	f_2 = 0.65 GHz	1.415GHz
Return loss (S_{11})	19.62 dB	38.17 dB	25.42 dB
Isolation (S_{41})	-25.86 dB	18.24 dB	-30.30 dB
Output 1 (S_{21})	-4.11 dB	-4.67 dB	-2.54 dB
Output 2 (S_{31})	-4.24 dB	-3.96 dB	-3.37 dB
Phase difference	-89.32°	87.3°	-90.03°

TABLE 5. MEASUREMENT RESULT OF THE BLC IN [11].

	Measurement		
	f_1 = 0.195 GHz	f_2 = 0.67 GHz	1.465GHz
S_{11} and S_{41}	Not provided		
Output 1 (S_{21})	-4.415 dB	-4.415 dB	-4.420
Output 2 (S_{31})	-4.212 dB	-4.212 dB	-3.903
Phase difference	-89.36°	-94.92°	88.615

From the experiment results, our fabricated TB BLC has a good performance. Compared to reference paper [11], two types of BLC have similar performance. However, our proposed BLC has a compact size.

For the result analysis, as is widely known, the LH parts are implemented from chip inductors and capacitors of surface-mount-technology (SMT). In practice, the self-resonant frequency (SRF) of SMT chip components, the parasitic effects from soldering, and the metalized via-holes set a high-frequency limit to the design. In addition, the chip element

values are pre-determined somewhat quantitatively by manufacturers. Therefore, if an arbitrary element value is required, designers should be prepared to accept the non-design values or rely on an additional tuning step. Nevertheless, these degrade the desirable performances of the circuits and systems. Considering all of these, our results are acceptable.

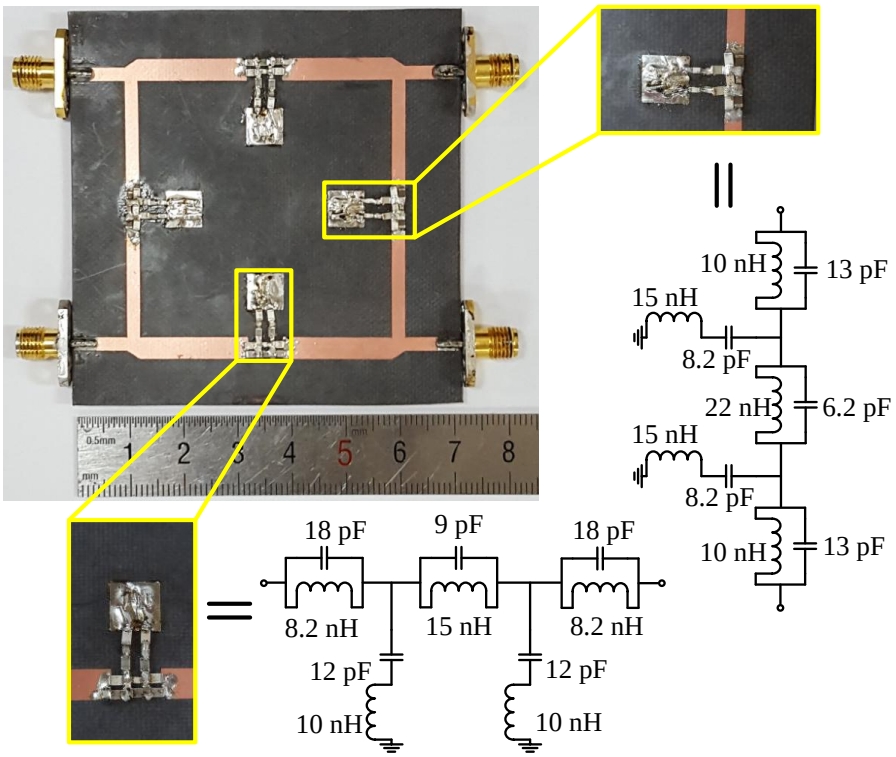

Figure 4.16 Fabricated TB BLC and used lump element values

Figure 6 shows a photograph of the fabricated DB BLC with one of the LH TL parts in detail. The size of the pure BLC circuit area is 47.0 ×46.5 mm^2. In order to compare the circuit size, we designed the BLC using the same tri-frequencies as those in [11]. The size

of the designed BLC by the previous method is 125×123 mm^2. The area of the fabricated circuit is only 14.2% compared to that of the previous method. Figure 4.17 shows a comparison in the size between the proposed DB BLC (fabricated photo) and the layout designed by [11].

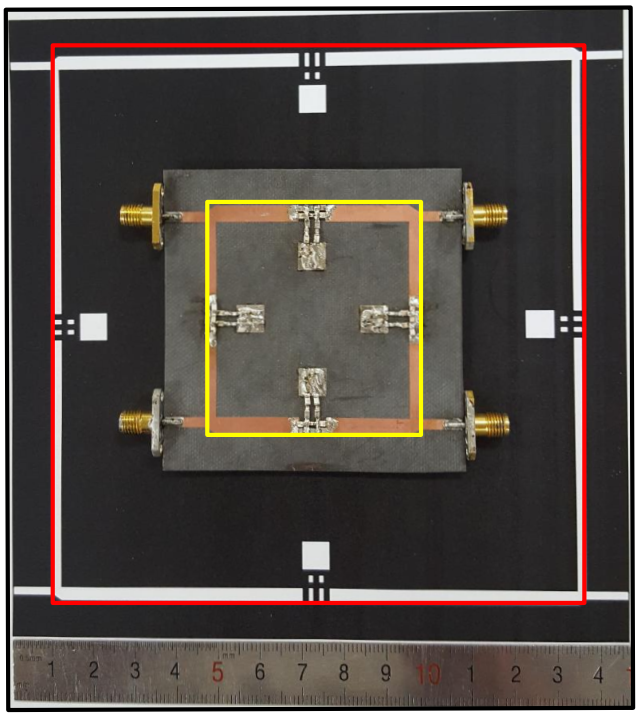

Figure 4.17 Comparison of the proposed DB BLC (fabrication) and previous work by [11] (CAD layout).

Chapter 5

Conclusion and future work

This chapter mainly discussed conclusion and discussion. Future work is presented in this chapter as well.

5.1 Conclusion and discussion

In this paper, the design of a compact TB BLC using DL CRLH is described. The size reduction theory has been analyzed and verified. The phase response group ($-\pi/4$, $\pi/4$,$-\pi/4$) at three operating frequencies is proved to be the best solution for a compact circuit size. Employing this structure, a TB microstrip BLC operating at 0.195 GHz, 0.67 GHz and 1.465 GHz is achieved, which has similar performance as previous work. However, the size of the proposed TB BLC is significantly compact, reduced by 85.8% compared to the previous TB BLC when they are both designed using DL CRLH TLs for the same TB frequencies. Simulated and measured results show good agreement, and the operating frequencies in all bands are well attained. This proposed TB BLC is significantly compact, and has steady performances due to the reliable realization, which is very useful in practical applications.

5.2 Future Work

The size reduction theory of CRLH is proposed in this thesis. As described in chapter 4, λ/4 length CRLH TL is widely used in microwave device design. Especially in [14], λ/4 length CRLH TL is applied as a resonator in band pass filter (BPF), which has a wide bandwidth and dual band operation. In the future, tri-band λ/4 length TL can be also applied in wide band TB BPF design.

Acknowledgment

The author extends his sincere thanks to BK21 plus's support.

I would also like to express my sincere appreciation to my academic advisor, Prof. Yongchae Jeong and Prof. Jongsik Lim all their help, support, guidance and providing me with the opportunity to study the interesting field of CRLH. Sincere thanks should also go to my thesis committee chairmen Prof. Haewon Son and Prof. Donggu Lim for their brilliant comments and suggestions. Special thanks should also go to the Microwave Circuit Design Lab members for creating a great atmosphere for study and research.

Thank you for always being there for me, my friends.

Last, but not least, I would like to thank my wonderful family for their continuous support and for providing me with the calm environment to work in.

Qi Wang

Jeonju, South Korea

References

[1] Veselago, V. G., "The electrodynamics of substances with simultaneously negative values of ε and μ," *Soviet Physics Uspekhi-Ussr*, Vol. 10, 509-514, Jan.-Feb. 1968.

[2] "Breakthrough of the year: The runners-up," *Science*, vol. 302, no.5653, pp. 2039–2045, 2003.

[3] C. Caloz and T. Itoh, Electromagnetic Metamaterials, Transmission Line Theory and Microwave Applications. New York: Wiley, 2005.

[4] I. H. Lin, M. D Vincentis, C. Caloz, and T. Itoh, "Arbitrary dual-band components using composite right/left-handed transmission lines," *IEEE Trans. on Microwave Theory and Techniques*, vol. 52, no. 4, pp.1142-1149, Apr. 2004.

[5] C. Caloz, "Dual composite right/left-handed (D-CRLH) transmission line metamaterial," *IEEE Mircowave and wireless components letters*, vol. 16, no.11, Nov. 2006.

[6] A. Rennings, T. Liebig, C. Caloz, and I. Wolff, "Double-Lorentz transmission line metamaterial and its application to tri-band devices," *IEEE MTT-S Int Microwave Symp*, Honolulu, HI , pp. 1427–1430, 2007.

[7] D.M. Pozar, Microwave engineering, Wiley, New York, 1998.

[8] Q. Wang, J. Lim and Y. Jeong, "Design of a compact dual-band branch line coupler using composite right/left-handed transmission lines," Electronic Letters, vol.52, no.8, pp. 630-631, Apr. 2016.

[9] C. Caloz and T. Itoh, “Transmission line approach of left-handed (LH) structures and microstrip realization of a low-loss broadband LH filter,” *IEEE Trans. Antennas Propagat.*, vol. 52, no.5, May 2004.

[10] C. Caloz and T. Itoh, “Application of the transmission line theory of left-handed (LH) materials to the realization of a microstrip LH transmission line,” *IEEE AP-S Int. Symp.* Dig., vol. 2, 2002, pp. 412–415.

[11] Hanseung Lee and Sangwook Nam, "Triband branch line coupler using double-lorentz transmision lines," *Mircrowave and Optical Technology Letters*, vol.50, no.5, May 2008.

[12] A. Kumar, Mobile TV, DVB-H, DMB, G3 systems and rich media applications, Butterworth-Heinemann, 2007.

[13] K. Iyer and G. V. Eleftheriades, “Negative refractive-index metamaterials supporting 2-D waves,” in *IEEE MTT-S Int. Microwave Symp. Dig.*, vol. 2, Seattle, WA, June 2002, pp. 1067–1070.

[14] G. Chaudhary1, Y. Jeong, and J. Lim, “A Broad-Bandwidth Dual-Band Bandpass Filter Design Using Composite Right/Left Handed Transmission Lines,” *J. of Electromagn. Waves and Appl.*, vol. 25, no. 12, pp. 2138-2147, 2011.

Abstract in Korean

요약

본 논문은 double-Lorentz (DL) composite right/left handed(CRLH) 전송선로를 이용한 소형 삼중대역 브랜치 라인 결합기 설계에 방안을 제시한다. CRLH 전송선로의 한unit은 설계 파라미터를 조절함으로서 삼중대역 동작주파수에서 각각 $-\pi/4$, $\pi/4$ 와 $-\pi/4$ 위상 값을 갖게 된다. 이 CRLH 전송선로를 이용해 0.195 GHz, 0.67 GHz 와 1.465 GHz 에서 동작하는 브랜치 라인 결합기(BLC)를 설계했다. 제안한 이중대역 BLC는 이전에 설계된 CRLH 구조를 이용한 이중대역 BLC 보다 좋은 성능과 작은 사이즈를 갖는다.

주요어: 삼중대역, 브랜치 라인 결합기, CRLH

Appendix: Matlab code

Solve the equation

```
clear all
clc
syms  CP LR  CL LP CR LL;
eq1='10^(-3)*2*pi*2500*0.195*CP+(2*pi*0.195*LR)/(1-(2*pi*0.
195)^2*LR*CL*10^(-3))=50*pi/4'; %ϕ1 can be modified here
eq2='10^(-3)*2*pi*2500*0.67*CP+(2*pi*0.67*LR)/(1-(2*pi*0.67
)^2*LR*CL*10^(-3))=-50*pi/4'; %ϕ2 can be modified here
eq3='10^(-3)*2*pi*2500*1.465*CP+(2*pi*1.465*LR)/(1-(2*pi*1.
465)^2*LR*CL*10^(-3))=50*pi/4'; %ϕ3 can be modified here
eq4='LR/CR=2.5';
eq5='LL/CL=2.5';
eq6='LP/CP=2.5';
S=solve(eq1,eq2,eq3,eq4,eq5,eq6);
%type"[double(S.LP) double(S.CP) double(S.LL) double(S.CL)
double(S.LR) double(S.CR)]" in command window to run.
```

Loop program to find the $\phi_{DL\,CRLH}$

```
clc
clear all
syms  CP LR  CL LP CR LL;

n12=zeros(1,6);% to store 6 parameters after find the right
values

V1=50*pi/4;
V3=50*pi/4;

for n=390:400

eq1=10^(-3)*2*pi*50^2*0.195*CP+(2*pi*0.195*LR)/(1-(2*pi*0.1
95)^2*LR*CL*10^(-3))-V1';
eq2=10^(-3)*2*pi*50^2*0.67*CP+(2*pi*0.67*LR)/(1-(2*pi*0.67)
^2*LR*CL*10^(-3))+50*(pi*0.1*n/180);
eq3=10^(-3)*2*pi*50^2*1.465*CP+(2*pi*1.465*LR)/(1-(2*pi*1.4
65)^2*LR*CL*10^(-3))-V3;
eq4=LR-CR*2.5;
eq5=LL-CL*2.5;
eq6=LP-CP*2.5;
S1=solve(eq1,eq2,eq3,eq4,eq5,eq6,'CP','LR','CL','LP','CR','
LL');
```

```
f=0.67;W=2*pi*f*10.^9;Z0=50;


LP1=S1.LP*1e-9;LR1=S1.LR*1e-9;LL1=S1.LL*1e-9;

CP1=S1.CP*1e-12;CR1=S1.CR*1e-12;CL1=S1.CL*1e-12;


phi=-W*sqrt(LP1*CP1)-atan((2*W*LR1.*(1-W.^2*LL1*CR1).*(2-2*

W.^2*LR1*CL1)-W.^3*LR1^2*CR1+W*Z0^2*CR1.*(2-2*W.^2*LR1*CL1)

.^2)./(2*Z0*(2-2*W.^2*LR1*CL1).^2.*(1-W.^2*LL1*CR1)-2*Z0*W.

^2*LR1*CR1.*(2-2*W.^2*LR1*CL1)));


newphi=double(vpa(phi));

n11(n)=newphi;

end
```

%type "n11" in command window to get n11 matrix, then find the right phase value and corresponding *n*.